

# Novel anti-inflammatory film as a delivery system for the external medication with bioactive phytochemical “Apocynin”

Hend Mohamed Anter<sup>1</sup>  
Irhan Ibrahim Abu Hashim<sup>1</sup>  
Walaa Awadin<sup>2</sup>  
Mahasen Mohamed Meshali<sup>1</sup>

<sup>1</sup>Department of Pharmaceutics,  
Faculty of Pharmacy, Mansoura  
University, Mansoura, Dakahlia, Egypt;

<sup>2</sup>Department of Pathology, Faculty  
of Veterinary Medicine, Mansoura  
University, Mansoura, Dakahlia, Egypt

**Purpose:** Recently, Apocynin (APO) has emerged as a bioactive phytochemical with potent antioxidant and anti-inflammatory properties. No reports have been published so far concerning its topical application as a pharmaceutical dosage form for prospective use. To the best of our knowledge, this is the first study to fabricate novel anti-inflammatory film for external medication with APO.

**Methods:** APO film was prepared using casein (CAS) as a natural protein film former by solvent casting technique. The medicated film was extensively evaluated in terms of its various physicochemical characteristics, ex vivo skin permeation profile, stability, and finally in vivo anti-inflammatory activity on carrageenan-induced rat paw edema.

**Results:** The film represented satisfactory mechanical properties along with good flexibility. Fourier transform-infrared spectroscopy, differential scanning calorimetry, and X-ray diffraction revealed possible solubility of APO in the amorphous CAS and inter- and intramolecular hydrogen bonding between the film components. The ex vivo skin permeation results of the medicated film demonstrated non-Fickian diffusion mechanism of the permeated drug. Application of APO film to rat paw before carrageenan-induced paw edema or after induction disclosed eminent anti-inflammatory activity expressed by marked decrease in paw swelling (%) and increase in edema inhibition rate (%). In addition, histopathologic examination revealed a significant decrease in inflammatory scores. The immunohistochemical expression levels of both nuclear factor kappa B and cyclooxygenase-2 were significantly suppressed.

**Conclusion:** These results indicated that CAS film could be applied as a promising external delivery system for the anti-inflammatory APO.

**Keywords:** Apocynin, casein, topical film, in vivo studies, inflammation, pharmacodynamics

## Introduction

Inflammation is fundamentally a complex biologic defense response of the body against injuries or harmful stimuli as infectious agents and irritants.<sup>1</sup> A diversity of dermatologic conditions is ranged according to the severity of inflammation from mild skin rash to severe dermatitis.

Currently, steroidal and nonsteroidal anti-inflammatory drugs (NSAIDs) are still the mainstay in treatment of inflammatory diseases. However, they are fraught with serious adverse effects that limited their application.<sup>2,3</sup> Even topical therapy with NSAIDs is facing some problems concerning their clinical effectiveness.<sup>4</sup> Therefore, seeking for other alternatives mainly from natural sources is a necessary urgent issue.

Apocynin (APO) (4-hydroxy-3-methoxyacetophenone) is a natural organic compound structurally related to vanillin. Hence, its other synonymous name is

Correspondence: Irhan Ibrahim  
Abu Hashim  
Department of Pharmaceutics, Faculty  
of Pharmacy – Mansoura University,  
El-Gomhoria Street, Mansoura,  
Dakahlia 35516, Egypt  
Tel +20 109 300 8481  
Fax +20 50 224 7496  
Email irhanabuhashim@hotmail.com

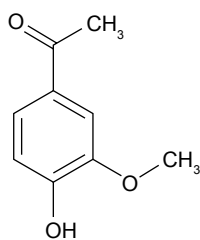


**Figure 1** Chemical structure of APO.  
**Abbreviation:** APO, Apocynin.

acetovanillone (Figure 1). It was originally isolated from the root of perennial herbaceous plant *Apocynum cannabinum* (Canadian hemp). Also, APO was extracted from the root of *Picrorhiza kurroa* (Scrophulariaceae) native to Himalayas.<sup>5</sup> According to successive intensive pharmacologic investigations on a variety of cell lines and animal models, APO was proved to be a bioactive phytochemical with potential antioxidant and anti-inflammatory properties.<sup>6–9</sup> This powerful efficacy is correlated to specific inhibition of nicotinamide adenine dinucleotide phosphate (NADPH) oxidase, an enzyme responsible for reactive oxygen species production, and other inflammatory mediators.<sup>10,11</sup>

Nowadays, medicated films have attracted a great considerable attention as a topical application therapy because of their feasible application, definite area with accurate dose, ability of therapy termination at anytime by removing the system, and improved patient compliance.<sup>12</sup> Polymeric film formers (natural or synthetic) represent the main backbone for film preparation and can be used alone or in combination with each other.<sup>12</sup>

Casein (CAS), a proline-rich protein, constitutes about 80% of the total proteins in milk. It is cheap, safe, available, highly stable, biocompatible, and biodegradable. Moreover, CAS has other characteristic features as binding to ions and small molecules, interaction with macromolecules, emulsification and self-assembly, as well as excellent gelation and water binding ability.<sup>13,14</sup> Owing to its structure and these unique physicochemical properties, CAS has been documented as a promising natural candidate for the preparation of conventional and novel pharmaceutical drug delivery systems.<sup>15–17</sup>

In spite of the wealthy literature data on the versatile pharmacologic effect of APO, no reports have been published so far concerning its topical application as a pharmaceutical dosage form. Thereby, this research was conducted to fabricate and extensively evaluate novel anti-inflammatory film as a dosage form for the external medication with the bioactive phytochemical APO using CAS as a natural protein film former.

## Materials and methods

### Materials

APO, carrageenan, benzalkonium chloride, and bovine serum albumin (BSA) were purchased from Sigma-Aldrich (St Louis, MO, USA). CAS-soluble light white was obtained from BDH biochemical, Australia. Glycerol was purchased from Adwic, EL-Nasr Pharmaceutical Chemicals Co. (Cairo, Egypt). All other chemicals and solvents were of analytical reagent grade.

### Solubility study of APO

The solubility study was performed in deionized water. Glass vials, each containing an excess amount of APO (200 mg) dispersed in 10 mL deionized water, were continuously shaken for 24 hours at  $(37 \pm 1^\circ\text{C})$  using a thermostatically controlled agitating water bath (Grant Instrument, Cambridge Ltd., UK). Vials were removed from the water bath, and the solutions were filtered using membrane filter ( $0.45 \mu\text{m}$ ), and the amounts dissolved in the filtrates were estimated spectrophotometrically at 272 nm (Spectro UV-VIS double beam, Labomed Inc., CA, USA).

### Preparation of APO film

APO film was prepared by solvent casting technique using CAS as a film-forming protein.<sup>18</sup> APO (0.05 g) was weighed accurately and dissolved in 30 mL deionized water for 3 hours at room temperature using magnetic stirrer (Heidolph, IL, USA), followed by the addition of benzalkonium chloride (0.01%) as a preservative. Next, CAS (0.5 g) was added to the drug solution and mixed thoroughly with magnetic stirrer for 30 minutes. Glycerol (0.8 g) was then added as a plasticizer and penetration enhancer, and the solution was left on magnetic stirrer for another 30 minutes. The whole solution was poured into a glass petri dish with area of  $28.27 \text{ cm}^2$  under magnetic stirring to ensure uniform distribution of the components and dried at  $37^\circ\text{C}$  in an oven for 48 hours. After drying, the film was observed and inspected for any possible imperfections upon its removal from the petri dish. Finally, the film was packed in aluminum foil and preserved in a desiccator for further evaluation tests. The film was cut to smaller ones with an area of  $1.77 \text{ cm}^2$  by cork borer for the forthcoming tests.

### Physicochemical characterization of APO film

#### Thickness

Micrometer screw gage (Mitutoyo, Japan) was used for measuring the thickness of the whole medicated film at five different positions, and the mean value was calculated.<sup>19</sup>

### Weight variation

The weight variation of the medicated films (1.77 cm<sup>2</sup> each) was calculated by weighing five individual ones.<sup>19</sup>

### Drug content

A medicated film of specified area (1.77 cm<sup>2</sup>) was transferred into a beaker containing 30 mL phosphate buffer (PB) pH 5.5 and ultrasonicated for 15 minutes using ultrasonic homogenizer (Ultrasonic homogenizer, 4710 Series, Cole-Parmer Instrument Co., Chicago, USA). Then, the whole content was stirred on magnetic stirrer for 3 hours, followed by centrifugation. The supernatant was filtered using 0.45 μm filters. Spectrophotometric analysis was employed to assay the drug content at 272 nm against blank solution of plain film. Average of three determinations was estimated.

### Folding endurance

The test was performed on three films (1.77 cm<sup>2</sup> each) and the folding endurance value was estimated by the number of times required for the film to be folded at the same place without breaking or cracking.<sup>19</sup>

### Mechanical properties of the film

Computerized tensile strength tester (Instron3345, ID: 3345 k2068, weight capacity: 5 kN, USA) was employed to determine the tensile strength, percentage elongation at break, and modulus of elasticity (Young's modulus) of both plain and medicated films. The sensitivity of the machine was in the range of 0–5,000 N (500 kg). It consists of two load cell grips: lower fixed one and upper movable one. Strips from the film with length of 4 cm and width of 2 cm were cut and fixed between these cell grips positioned at a distance of 4 cm representing the length of the film. A speed of 50 mm min<sup>-1</sup> was applied to all measurements. At specific rate, the load applied to the film was automatically increased until breakage of the film. The mechanical properties of the film were calculated using computerized tensile strength tester according to the following equations<sup>18</sup>:

The percentage elongation at break,  $E_b$ , of tested films was determined as follows:

$$E_b = \frac{L - L_o}{L_o} \times 100 \quad (1)$$

where  $L$  is the final length of the film and  $L_o$  is its original length.

The modulus of elasticity ( $M_E$ ) of the film was calculated according to Hook's law:

$$B = M_E \left( \frac{L - L_o}{L_o} \right) \quad (2)$$

The tensile strength,  $B$ , of tested films was calculated according to the following equation:

$$B = \frac{F}{A} \quad (3)$$

where  $F$  is the maximum force exposed to the film and  $A$  is its cross-sectional area.

### Surface pH

The medicated film (1.77 cm<sup>2</sup>) was allowed to swell by keeping it in contact with 1 mL distilled water for 2 hours at room temperature. pH indicator paper was used to measure the surface pH of the swollen film by comparing the change in color with that of standard color scale.<sup>20</sup>

### Moisture content

A weighed medicated film ( $W_i$ ) of area 1.77 cm<sup>2</sup> was kept in a desiccator containing activated silica at room temperature. The film was periodically weighed until a constant weight was achieved ( $W_f$ ). Calculation of the moisture content (%) was based on the following equation:<sup>21</sup>

$$\text{Moisture content (\%)} = \frac{W_i - W_f}{W_i} \times 100 \quad (4)$$

where  $W_i$  is the initial weight of the film and  $W_f$  is the final weight of the film.

### Moisture uptake

The medicated film (1.77 cm<sup>2</sup>) was kept in a desiccator containing activated silica at room temperature for 24 hours and weighed ( $W_i$ ). Thereafter, the film was transferred into another desiccator containing saturated NaCl solution (relative humidity, RH 75%) at room temperature till a constant weight was attained ( $W_f$ ). The moisture uptake (%) was calculated according to the following equation:<sup>22</sup>

$$\text{Moisture uptake (\%)} = \frac{W_f - W_i}{W_i} \times 100 \quad (5)$$

where  $W_i$  is the initial weight of the film and  $W_f$  is the final weight of the film.

### Swelling property

Briefly, the swelling characteristic of the medicated film (1.77 cm<sup>2</sup>) was estimated by initially weighing the film ( $W_i$ ) and then placing it in a petri dish containing 5 mL PB (pH 5.5) at 37°C to give a chance for imbibition. At specific time intervals, the film was removed and excess buffer solution on its surface was gently wiped with filter paper. The swollen film was reweighed ( $W_t$ ) and the swelling ratio, SR, was calculated according to the following equation:<sup>23</sup>

$$SR = \frac{W_t - W_i}{W_i} \quad (6)$$

where  $W_t$  is the weight of the film at time  $t$ , and  $W_i$  is the initial weight of the film.

### Fourier transform-infrared (FT-IR) spectroscopy

The FT-IR spectra of APO, CAS, their physical mixture (1:10, respectively), as well as plain and medicated films were recorded using FT-IR spectrophotometer (Madison Instruments, Middleton, WI, USA). Discs of each sample (2 mg) individually with 200 mg KBr were scanned over a wave number range of 4,000–500 cm<sup>-1</sup>.

### Differential scanning calorimetry (DSC)

Thermal analysis of the drug, CAS, their physical mixture (1:10, respectively), as well as plain and medicated films was carried out using DSC (DSC 6000; Perkin-Elmer, Waltham, MA, USA). Hermetically sealed aluminum pans containing samples (4 mg per sample) were heated over a temperature range of 30°C–350°C at a heating rate of 10°C/min under constant nitrogen purging at 20 mL/min. Indium was used as a reference standard for temperature calibration.

### X-ray diffractometry (XRD)

X-ray diffraction patterns of the drug, CAS, their physical mixture (1:10, respectively), as well as plain and medicated films were detected using X-ray diffractometer (Diano Corp., Woburn, MA, USA) equipped with Cu K $\alpha$ . The analysis was carried out at 45 kV and 9 mA corresponding to the voltage and current used, respectively, at a 2 $\theta$  angle.

### Scanning electron microscopy (SEM)

The surface morphology of APO, CAS, their physical mixture (1:10, respectively), plain film and medicated film, before and after ex vivo skin permeation experiment, was investigated

using an SEM (JSM 6150, JEOL, Tokyo, Japan) operated at an acceleration voltage of 20 kV. The samples were mounted on stubs and coated with gold palladium alloy by the JFC-1200 Fine Coater (JEOL, Tokyo, Japan). Photographs were captured at the proper magnification.

### Ex vivo skin permeation study

All animal experiments and preparation of skin samples were conducted after approval from the Scientific Committee of the Faculty of Pharmacy, Mansoura University, Egypt, in accordance with the Principles of Laboratory Animal Care NIH publication, 1985 revision.

Vertical Franz diffusion cell was used for ex vivo permeation study. Excised abdominal skin of newly born male Wistar albino rats (2 weeks old) was used after careful removal of adhering subcutaneous fats and visceral debris. The skin was examined for its integrity. It was thoroughly washed with distilled water, saline, and finally equilibrated with PB (pH 7.4) for 24 hours at refrigerated temperature (4  $\pm$  1°C) before starting the experiment. Then, the excised skin was mounted between the donor and receptor compartments of the diffusion cell with the stratum corneum side facing the donor one. The receptor compartment with a permeation area of 1.77 cm<sup>2</sup> was filled with 10 mL PB (pH 7.4). The medicated film with an area of 1.77 cm<sup>2</sup> was tightly adhered to the stratum corneum of the skin by hydration with 0.5 mL of the buffer solution. The receptor buffer solution was constantly and continuously stirred with thermostatically controlled shaker water bath (Gallenkamp BKS-350, E.E.C.) adjusted at 100 rpm/min and maintained at 37  $\pm$  0.5°C. The drug concentration was measured spectrophotometrically at 278 nm. The same steps were accomplished using plain film as a blank to abolish any possible interferences related to rat skin or film components. The amount of APO that permeated the rat skin per unit surface area was plotted against time. The steady-state flux ( $J_{ss}$ ) ( $\mu$ g/cm<sup>2</sup>/h) was calculated from the slope of the linear portion of the plotted permeation curve, and the permeability coefficient ( $K_p$ ) (cm/h) was estimated by dividing the flux over the drug concentration in the donor compartment.<sup>24</sup>

### Kinetic modeling of drug release data

To ascertain the mechanism of APO release from the prepared CAS film, the ex vivo release data were fitted to numerous mathematical models like zero-order, first-order, Higuchi,<sup>25</sup> and Korsmeyer–Peppas equation:<sup>26</sup>

$$\frac{m_t}{m_\infty} = kt^n \quad (7)$$

where  $m_t/m_\infty$  is the fraction of drug released,  $k$  is the kinetic constant,  $t$  is the release time, and  $n$  is the diffusional exponent for drug release that equals the slope of  $\log m_t/m_\infty$  vs  $\log$  time curve. The model representing correlation coefficient ( $r^2$ ) with the highest value was considered to depict the drug release from CAS film.

### Stability study

The stability studies of APO/CAS film were carried out at different temperatures:  $25 \pm 2^\circ\text{C}$  ( $60 \pm 5\%$  RH) and  $4 \pm 1^\circ\text{C}$  for 6 months. The films were wrapped up in aluminum foil throughout the study and evaluated every 2 months with regard to their ex vivo skin permeation profiles, skin permeation parameters ( $J_{ss}$  and  $K_p$ ), and drug content (%).

### In vivo studies

Male Wistar albino rats weighing 100–150 g were used for the subsequent in vivo skin irritation and anti-inflammatory activity experiments. The animals were housed individually in separate cages under standard laboratory conditions (temperature of  $25 \pm 1^\circ\text{C}$ , RH of  $55 \pm 5\%$ , and photoperiod of 12-hour light:12-hour dark cycles) with free access to diet and water.

### Skin irritation study

The dorsal hair of the rats was shaved by an animal hair clipper 24 hours before starting the study. The animals were divided into three groups (six animals/group). Group I served as a control (without any treatment) and group II treated with formalin aqueous solution (0.8% v/v) as a standard irritant.<sup>27</sup> Medicated films were attached to the back of the animals of group III by Tegaderm (3M Health Care, USA). The application of either medicated film or formalin solution was repeated three times per day. Finally, the animals were killed and the treated skin areas were dissected out for histologic examination after H&E staining using light microscope (Olympus, Tokyo, Japan).

## Pharmacodynamic studies

### Carrageenan-induced rat paw edema

The anti-inflammatory activity of APO topical film was assessed according to the previously reported carrageenan-induced rat paw edema model.<sup>28</sup> Briefly, the rats were divided into four groups with six animals per group. The first one served as a control (without any treatment). The second one was injected with carrageenan only. The third one served as a pretreated group (treatment with the medicated film of area  $1.77\text{ cm}^2$  containing 3.05 mg APO 5 hours before carrageenan injection) because preliminary study showed that 5 hours of

the film application before carrageenan injection was enough for the drug to produce its pharmacodynamic effect. The fourth one served as a post-treated group (treatment with similar medicated film after half an hour of carrageenan injection). The film was moistened with 30  $\mu\text{L}$  deionized water, then secured firmly with the rat paw by Band-Aid® (Brand Adhesive Bandages SKIN-FLEX). Acute inflammation was induced by subplantar injection of 0.1 mL freshly prepared carrageenan solution in normal saline (1% w/v) into right hind paw of each rat.

The paw thickness was measured by a digital vernier caliper (Elora, Germany) just before carrageenan injection and thereafter at 1, 3, 5, 7, and 24 hours. The paw swelling (%) and edema inhibition rate (%) were calculated and plotted against each time interval:<sup>29</sup>

$$\text{Paw swelling (\%)} = \frac{b-a}{a} \times 100 \quad (8)$$

where  $a$  is the hind paw thickness prior to edema induction and  $b$  is the hind paw thickness at different times post-induction.

$$\text{Edema inhibition rate (\%)} = \frac{E_c - E_t}{E_c} \times 100 \quad (9)$$

where  $E_c$  is the average paw swelling of group received carrageenan only and  $E_t$  is the paw swelling of the treated group with the medicated film.

### Histologic and immunohistochemical (IHC) studies

Animals from the above-mentioned experiment were killed, and 10% formalin was employed to fix the excised soft paw tissues for 24 hours followed by paraffin embedding. Two sets of sections were cut at 5  $\mu\text{m}$  thickness. One set of sections was stained with H&E according to Bancroft and Gamble.<sup>30</sup> The sections stained by H&E were scored from 0 to 5 according to the inflammation degree as follows: no inflammation = 0, mild inflammation = 1, mild/moderate inflammation = 2, moderate inflammation = 3, moderate/severe inflammation = 4, and severe inflammation = 5.<sup>31,32</sup>

The other set of sections was immunostained for studying expression levels of cyclooxygenase-2 (COX-2) and nuclear factor kappa B (NF- $\kappa\text{B}$ ) in treated and untreated animals using EnVision method according to the manufacturer's recommendations (Thermo Fisher Scientific, Waltham, MA, USA). Following deparaffinization and dehydration, the tissue sections were exposed to microwave oven treatment in 0.01 mol/L sodium citrate buffer (pH 6.0) for 8 minutes

at 600 W. The endogenous peroxidase was blocked by application of 0.3% H<sub>2</sub>O<sub>2</sub> on tissue sections for 30 minutes. After washing with PBS pH 7.4, the sections were incubated at 4°C overnight with the primary antibody: anti-COX-2 (1:50) and anti-NF-κB (1:100) in PBS containing 1% BSA. After triple rinsing with PBS, the sections were treated with biotinylated anti-immunoglobulin for 1 hour at room temperature, then washed again and reacted with the streptavidin–biotin system by using 0.04% 3, 3'-diaminobenzidine tetrahydrochloride for 1 minute as chromogen. Negative control was established by replacing the primary antibody with PBS.

The sections treated for immunostaining were scored from 0 to 3 as follows: absent staining = 0, weak staining = 1, moderate staining = 2, and strong staining = 3.<sup>33</sup> Such scoring clearly reflected the capability to realize the positive reactions under high, medium, and low-power microscopic magnifications.

### Statistical analysis

Graphpad prism software version 5.00 (GraphPad Software, Inc., La Jolla, CA, USA) was utilized to carry out the statistical processes. Data distribution was checked by Kolmogorov–Smirnov test and revealed normal distribution. Statistical analysis was proceeded by one-way analysis of variance followed by Tukey–Kramer multiple-comparisons test. The significant statistical differences were considered at  $P < 0.05$ .

Sample size was calculated by resource equation method, which is applicable to animal experiments according to the following equation:<sup>34</sup>

$$E = \frac{\text{Total number of animals} - \text{Total number of groups}}{\text{Total number of groups}} \quad (10)$$

when E value lies between 10 and 20, it represents an adequate sample size.

In our study, we conducted the animal experiments on four groups (six animals per group). So,  $E = (6 \times 4) - 4 = 20$ . Hence, the value of E equals 20, which is in the acceptable limit and indicates an adequate sample size.

## Results and discussion

### Preparation of APO film

The solubility of APO was found to be 2 mg/mL in deionized water. Preliminary trial showed that CAS film consisting of 0.5 g CAS, 0.05 g APO, and 0.8 g glycerol was acceptable with respect to consistency. Glycerol has dual function as plasticizer and penetration enhancer.<sup>35</sup> Addition of different

surface-active agents such as transcutool, propylene glycol, and Tween 80 to increase the solubility of the drug and its penetration through the skin resulted in a very soft film.

### Physicochemical characterization of APO film

#### Appearance, thickness, weight variation, and drug content

Visual and tactile inspection of the prepared medicated film demonstrated its elegant appearance, homogeneity, and smooth surface without any signs of cracking.

The measured thickness ( $0.352 \pm 0.013$  mm), weight ( $93.8 \pm 1.5$  mg), and drug content ( $97.33 \pm 0.72\%$ ) of the films with minimum SD values ascertained their good uniformity and accuracy of drug distribution.

#### Mechanical properties and folding endurance of the film

The folding endurance, tensile strength, percentage elongation, and modulus of elasticity (Young's modulus) values for plain and medicated films were determined for assessment of their mechanical properties and flexibility. No significant difference in properties was noticed between plain and medicated films. The films presented folding endurance value greater than 300 times at the same place without cracks as well as satisfactory data of tensile strength, percentage elongation, and modulus of elasticity in both plain and medicated ones (Table 1).

These results revealed that the prepared film possessed appropriate mechanical properties along with good flexibility that would preserve its integrity with general skin folding upon application. The addition of glycerol as a plasticizer in CAS film rendered it more flexible through increasing the free volume of the polymer network as a result of decreasing the intermolecular hydrogen bonding between the polar groups of adjacent CAS molecules. Also, glycerol afforded the CAS film with reasonable tensile strength and elasticity under normal conditions.<sup>36</sup>

#### Surface pH

The surface pH of the medicated film was  $6.0 \pm 0.5$  indicating its compatibility with skin pH and, hence, its suitability

**Table 1** Mechanical parameters of plain and medicated films

Formula	Elongation (%)	Tensile strength (kg/mm <sup>2</sup> )	Modulus of elasticity (kg/mm <sup>2</sup> )
Plain film	24.896±4.837	0.005±0.002	0.035±0.008
Medicated film	28.021±3.881	0.008±0.002	0.056±0.012

**Note:** Each value represents the mean ± SD (n=3).

for topical application without any susceptibility to skin irritation.<sup>37</sup>

### Moisture content and moisture uptake

Moisture content and moisture uptake studies gave an insight regarding the film stability. The moisture content (%) of the medicated film was low ( $1.429 \pm 0.113\%$ ), which could help in maintaining its stability as well as preventing its dryness and brittleness throughout long-term storage especially under dry conditions. On the other hand, the medicated film exhibited a relatively high moisture uptake (%) of  $13.506 \pm 0.918\%$ , which could be attributed to the hygroscopicity of glycerol and moisture sensitivity of CAS by the presence of their polar groups.<sup>38</sup> Nevertheless, this value of moisture uptake is still satisfactory and indicates the film ability to absorb wound and inflammatory exudates.<sup>23,39</sup>

### Swelling property

The swelling behavior of APO film was investigated by measuring the increase in weight at time intervals over 5 hours as shown in Figure 2. Maximum swelling of the film was noticed during the first 1-hour interval followed by gradual decrease up to 5 hours. The interaction between the polar groups of CAS molecules with that of water led to chain relaxation of polymeric segments that accounted for the overall swelling behavior.<sup>23</sup> However, the subsequent gradual decrease in film swelling might be correlated to the possibility of its erosion.

### FT-IR spectroscopy

FT-IR spectra of CAS, APO, their physical mixture, and plain and medicated films are demonstrated in Figure 3A. CAS typically showed characteristic bands at 3,423, 1,654, 1,523, and 1,242  $\text{cm}^{-1}$  corresponding to N-H stretching and

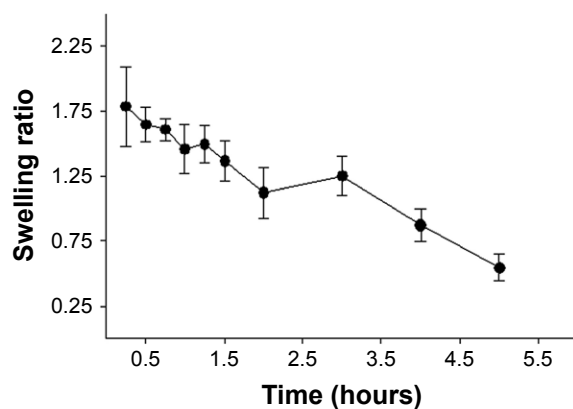


**Figure 2** The swelling behavior of the medicated film.  
**Note:** Each point represents the mean  $\pm$  SD ( $n=3$ ).

amide bending vibrations.<sup>40</sup> A band for CAS at 1,399  $\text{cm}^{-1}$  could be assigned to the carboxylate group (O-C-O).<sup>41</sup> The spectrum of APO disclosed all the distinctive bands of its functional groups: 3,384 (phenyl-OH), 3,007 (aromatic -H), 2,937 (alkane C-H), 2,843 (alkane C-H), and 1,660  $\text{cm}^{-1}$  (ketone C=O).<sup>42</sup> The spectrum of the physical mixture of both APO and CAS was similar to that of CAS, which might be attributed to dilution of the drug by the protein. In case of plain and medicated films, a broad band was observed in the region of 3,000–3,600  $\text{cm}^{-1}$ , which might refer to the free -NH groups, hydroxyl groups, and inter- and intramolecular hydrogen bonding between the film components.

### DSC

The respective DSC thermograms of CAS, APO, their physical mixture, and plain and medicated films are shown in Figure 3B. The thermogram of CAS exhibited a broad endothermic peak at 82.16°C related to the moisture evolution from the sample.<sup>41</sup> Additionally, two endothermic peaks were detected at 298.41°C and 313.28°C attributed to the degradation of CAS backbone.<sup>23</sup> The natural crystalline state of APO was manifested by distinguished melting peak at 116.91°C. In case of physical mixture, the characteristic endothermic peaks of both CAS and APO were observed at their authentic locations. The thermograms of plain and medicated films were almost coincided with each other. The peaks at 82.16°C corresponding to the presence of moisture in CAS disappeared with the appearance of new ones, which could be referred to glycerol. The thermogram of plain film without glycerol was similar to that of CAS alone (Figure S1). The disappearance of APO peak at 116.91°C from the medicated film might be due to the solubility of APO in CAS matrix during the preparation. The role of glycerol as nucleation inhibitor cannot be ignored.

### XRD

From the XRD data (Figure 3C), CAS pattern indicated its amorphous nature.<sup>43</sup> The pure APO showed high crystallinity with prominent diffraction peaks at  $2\theta$  of 6.64, 13.21, 14.43, 21.78, 22.67, 26.18, and 26.50. The physical mixture of CAS and APO as well as plain film experienced the same XRD pattern as CAS alone. A strong reduction in the crystallinity of APO was noted in the medicated film. The results of DSC and XRD investigations demonstrated the solubility of the drug in the amorphous CAS.

### SEM

Figure 4 elucidates the SEM micrographs of CAS, APO, their physical mixture, plain film, and medicated one before

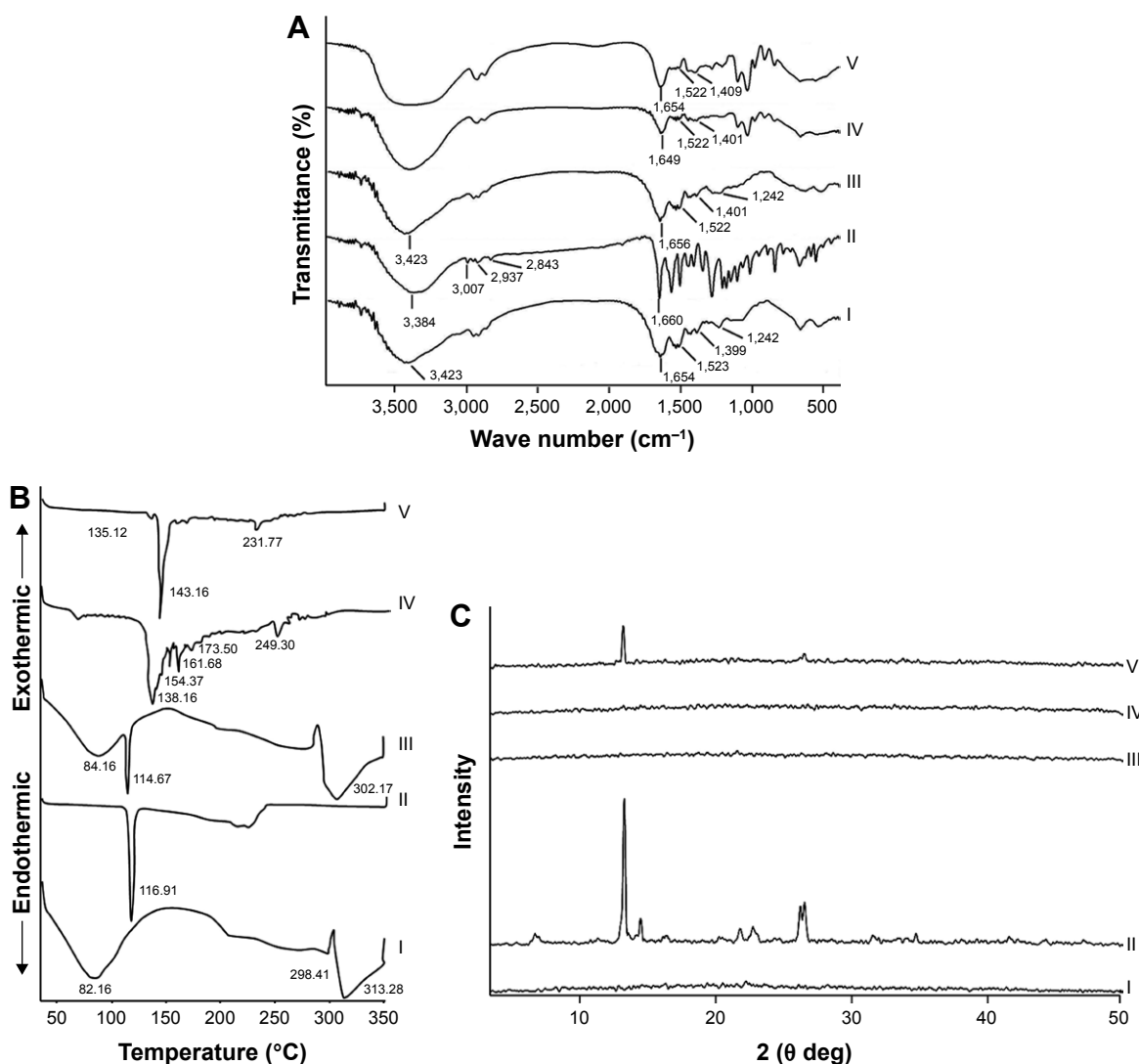


**Figure 3** FT-IR spectra (A), DSC thermograms (B), and XRD patterns (C).

**Note:** (I) CAS, (II) APO, (III) physical mixture, (IV) plain film, and (V) medicated film.

**Abbreviations:** APO, Apocynin; CAS, casein; DSC, differential scanning calorimetry; FT-IR, Fourier transform-infrared spectroscopy; XRD, X-ray diffractometry.

and after ex vivo skin permeation experiment. The crystals of APO were apparently irregular in shape and size as well as being much smaller than CAS particles. Their physical mixture displayed the existence of both particles. The surface of the plain film was smoother compared with that of the medicated one before ex vivo skin permeation study. The surfaces of both films were dense, and compact without distinct pores. After the ex vivo skin permeation experiment, the surface of the medicated film became relatively rough and porous because of drug diffusion from the film matrix. The medicated film might be considered as scaffold for external application of the drug.

### Ex vivo skin permeation data

Figure 5 shows the dynamic release of APO in PB pH 7.4 from film containing 0.05 g of the drug. To investigate the

influence of drug concentration on the release behavior, other films with 0.03 and 0.04 g of APO were included in the study. The results demonstrated a direct proportional increase in the rate of drug permeated through excised rat skin with the increase in the drug concentration. These data were substantiated by a significant increase in  $J_{ss}$  ( $20.10 \pm 3.761 \mu\text{g}/\text{cm}^2/\text{h}$ ) and  $K_p$  ( $12.00 \times 10^{-3} \pm 0.002 \text{ cm}/\text{h}$ ) of the medicated film containing 0.05 g of APO compared with the other ones ( $J_{ss}$  of  $10.95 \pm 1.507 \mu\text{g}/\text{cm}^2/\text{h}$  and  $K_p$  of  $9.00 \times 10^{-3} \pm 0.001 \text{ cm}/\text{h}$  for the film loaded with 0.04 g APO as well as  $J_{ss}$  of  $5.23 \pm 1.096 \mu\text{g}/\text{cm}^2/\text{h}$  and  $K_p$  of  $5.00 \times 10^{-3} \pm 0.001 \text{ cm}/\text{h}$  for the film loaded with 0.03 g APO). This could be simply explained on the basis that high drug concentration in the film resulted in a higher concentration gradient across the interface and, hence, a higher release rate was noticed. Similar findings were reported in case

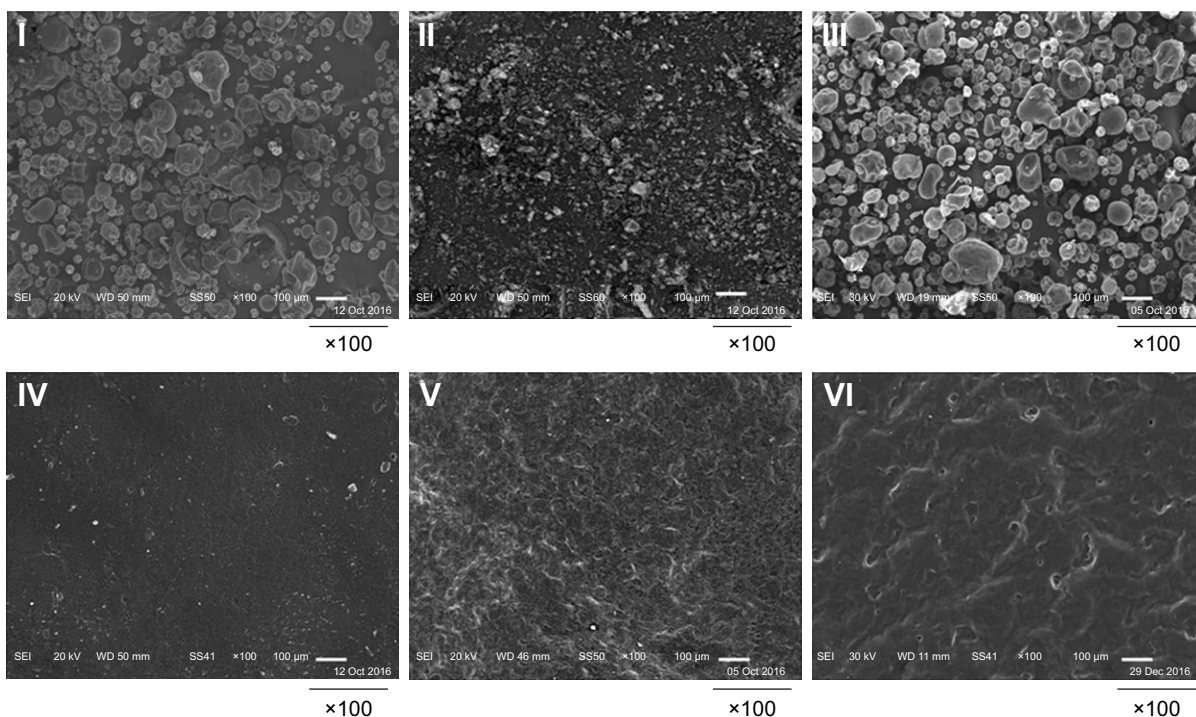


**Figure 4** SEM micrographs.

**Note:** (I) CAS, (II) APO, (III) physical mixture, (IV) plain film, (V) medicated film before ex vivo permeation study, and (VI) medicated film after ex vivo permeation study.

**Abbreviations:** APO, Apocynin; CAS, casein; SEM, scanning electron microscopy.

of gentamicin sulfate release from alginated dialdehyde-crosslinked CAS films.<sup>16</sup>

### Kinetic modeling of drug release data

To explore the mechanism of APO release from the CAS film and permeation through excised rat skin, different well-known kinetic models namely zero-order, first-order, and Higuchi model were applied. According to the  $r^2$  values,

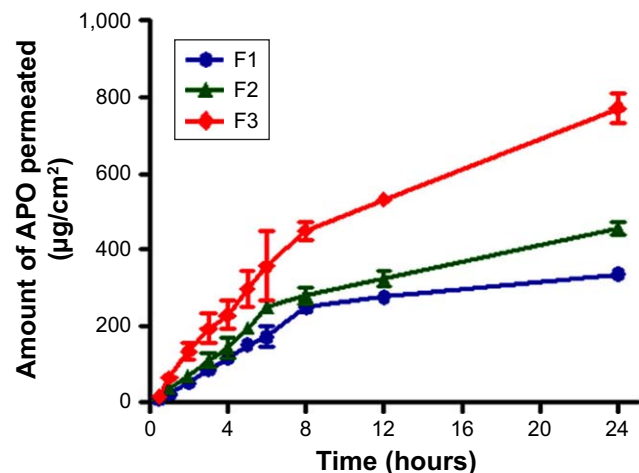


**Figure 5** Ex vivo skin permeation profiles of APO from the medicated film containing different drug concentrations.

**Notes:** (F1) 0.03, (F2) 0.04, and (F3) 0.05 g. Each point represents the mean  $\pm$  SD ( $n=3$ ).

**Abbreviation:** APO, Apocynin.

it was evident that the best fit followed Higuchi model ( $r^2=0.9681$ ) compared to zero-order ( $r^2=0.8898$ ) and first-order ( $r^2=0.9342$ ) indicating that the film released the drug by diffusion-controlled mechanism.

To examine more precisely the mechanism of APO release from the medicated film, semi-empirical Korsmeyer–Peppas equation was utilized to analyze the ex vivo permeation data. A profound look at the release exponent value ( $n=0.9722$ ) disclosed a non-Fickian (anomalous)-dominated mechanism governed by both diffusion and erosion.

### Stability study

The scope of our work was designed to carry out stability study for 6 months at two different storage conditions: refrigerated ( $4 \pm 1^\circ\text{C}$ ) and room ( $25 \pm 2^\circ\text{C}/60 \pm 5\% \text{RH}$ ) temperatures normally agree with the patient compliance for feasible daily use and storage conditions. Particularly, previous reported accelerated stability study on medicated CAS film at  $40 \pm 2^\circ\text{C}$  and  $75 \pm 5\% \text{RH}$  for 3 months revealed its physicochemical stability and efficacy.<sup>17</sup> Indeed, the thermal stability of CAS film is highly ascribed to the high number of proline peptides in CAS structure that leads to disruption of alpha helices and beta sheets as well as lack of disulfide bridges in their structure. As a consequence, CAS possesses relatively few secondary or tertiary structures, which give rise to its quite high heat stability.<sup>15</sup>

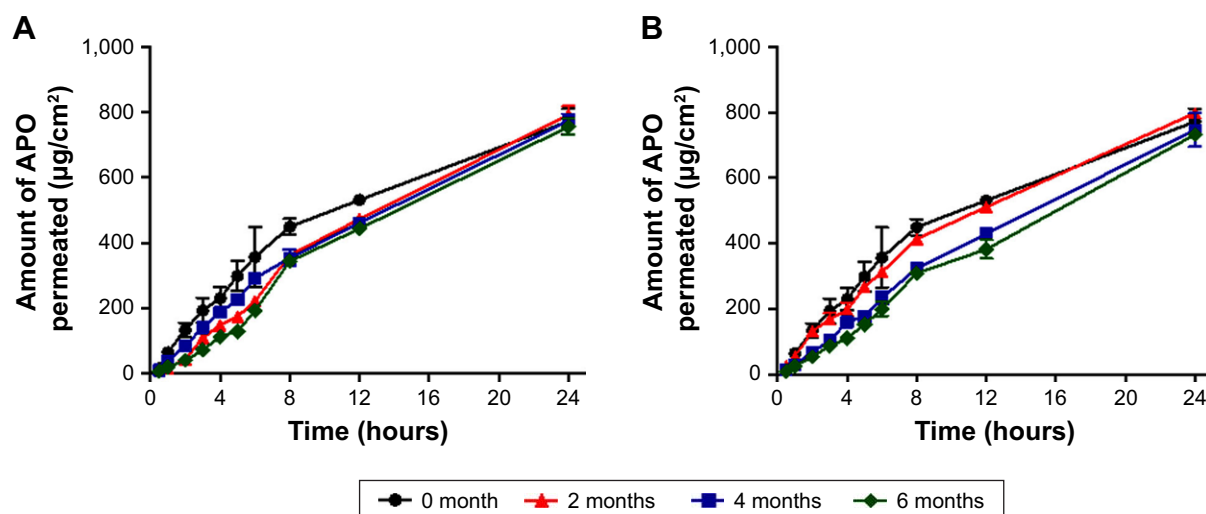


**Figure 6** Ex vivo skin permeation profiles of APO from the medicated film after storage for 6 months.

**Notes:** (A) Refrigerated temperature ( $4 \pm 1^\circ\text{C}$ ) and (B) room temperature ( $25 \pm 2^\circ\text{C}/60 \pm 5\% \text{RH}$ ). Each point represents the mean  $\pm$  SD ( $n=3$ ).

**Abbreviations:** APO, Apocynin; RH, relative humidity.

As graphically illustrated in Figure 6 and depicted in Table 2, no significant changes ( $P>0.05$ ) were observed in the ex vivo permeation profiles, skin permeation parameters ( $J_{ss}$  and  $K_p$ ), or drug content (%) of APO throughout the storage period at both temperatures, thus highlighting the stability of the medicated film.

## In vivo studies

### Skin irritation study

Skin irritation experiment was conducted as a prime prerequisite to estimate the potential of any irritation susceptibility of the prepared APO film. According to the histopathologic examination, rat skin treated with formalin (0.8% v/v) as a standard irritant showed focal loss of epidermal cells and hyalinization in superficial dermal connective tissue (Figure 7B) when compared to normal skin control group (Figure 7A). Noteworthy, the skin still retained its normal histopathologic integrity after topical application of APO film (Figure 7C). These results support the cutaneous safety and biocompatibility of the medicated film as well as its

prospective patient tolerability and acceptability for therapeutic use.

### Carrageenan-induced rat paw edema

In the present study, the carrageenan-induced rat paw edema as a commonly documented acute inflammatory model for studying the pathogenesis and therapeutic pathway of inflammatory diseases was employed to evaluate the anti-inflammatory effect of APO film.

As illustrated in Figure 8A, subplantar injection of right hind paw of rats with carrageenan manifested a biphasic time-dependent swelling. An uprising increase in paw swelling (%) up till nearly 7 hours was noticed. After that, minor elevation in paw swelling values was evident up till 24 hours. Pre- as well as post-treated regimens with APO film experienced the same pattern but “as expected” with comparatively lower values of percentage paw swelling. Figure 8B illustrations coincided with that of Figure 8A. The degree of inhibition of edema started with high percentage initially and the values decreased by time. Nearly,

**Table 2** Storage stability data of the medicated film at refrigerated ( $4 \pm 1^\circ\text{C}$ ) and room ( $25 \pm 2^\circ\text{C}/60 \pm 5\% \text{RH}$ ) temperatures

Parameters	Refrigerated temperature ( $4 \pm 1^\circ\text{C}$ )				Room temperature ( $25 \pm 2^\circ\text{C}/60 \pm 5\% \text{RH}$ )		
	0 month	2 months	4 months	6 months	2 months	4 months	6 months
$J_{ss}$ ( $\mu\text{g}/\text{cm}^2/\text{h}$ )	$20.10 \pm 3.761$	$26.74 \pm 1.180$	$26.16 \pm 2.409$	$25.80 \pm 1.229$	$23.99 \pm 0.784$	$26.43 \pm 3.301$	$27.08 \pm 0.890$
$K_p$ ( $\text{cm}/\text{h}$ ) $\times 10^{-3}$	$12.00 \pm 0.002$	$16.00 \pm 0.001$	$15.00 \pm 0.001$	$15.00 \pm 0.001$	$14.00 \pm 0.001$	$16.00 \pm 0.002$	$16.00 \pm 0.001$
Drug content (%)	$97.33 \pm 0.722$	$97.10 \pm 1.905$	$96.57 \pm 0.185$	$95.14 \pm 0.698$	$97.23 \pm 0.554$	$95.51 \pm 0.845$	$94.96 \pm 0.320$

**Note:** Each value represents the mean  $\pm$  SD ( $n=3$ ).

**Abbreviations:**  $J_{ss}$ , steady state flux;  $K_p$ , permeability coefficient; RH, relative humidity.

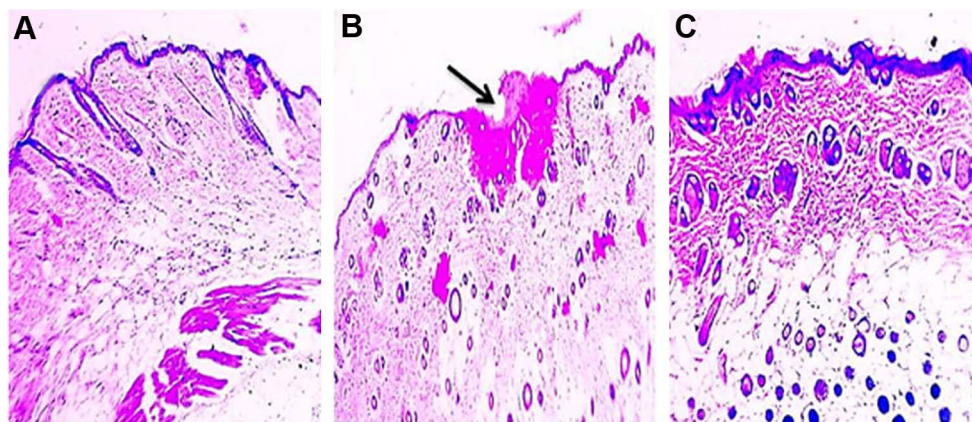


**Figure 7** Photomicrographs of histopathologic examination of skin irritation study.

**Notes:** Skin shows (A) normal histology in control group, (B) focal loss of epidermal cells, and hyalinization in superficial dermal connective tissue (arrow) after application of formalin aqueous solution (0.8% v/v) as a standard irritant, and (C) normal histologic features after triple application of the medicated film for 1 day. H&E, 100 $\times$ .

the percentage inhibition at 7 hours of once application of the film dropped to 50% of its initial value. Intuitively, this result necessitates the repeated application of medicated film every 7 hours. These data confer preliminary indication for the anti-inflammatory activity of APO film, which would be further substantiated after histologic analysis of the inflamed rat paw edema tissues.

## Histologic analysis of tissues from rat paw edema

Histologic evaluation of the anti-inflammatory effect of pre- and post-treatment regimens on rat paw edema tissues

In case of carrageenan-injected group without APO treatment, after 7 hours, paw tissue showed vacuolar and hydropic

degenerative changes in epidermal cells with marked inflammatory reaction characterized by massive accumulation of infiltrated neutrophils in dermis and subcutaneous muscles when compared to the control group (without induction of inflammation). After 24 hours, paw tissue revealed blisters formation with more severe inflammatory reaction as shown in Figure S2. Interestingly, the degenerative changes in epidermal cells were absent in pre- and post-treated groups within 7 hours after carrageenan injection with superiority for post-treated animals (Figures S3 and S4). Therefore, it was inferred that post-treatment regimen could be selected for further investigations with the film to be topically applied three times per day: first application (half an hour after carrageenan injection), second application (after 7 hours of injection), and third application (after 14 hours of injection).

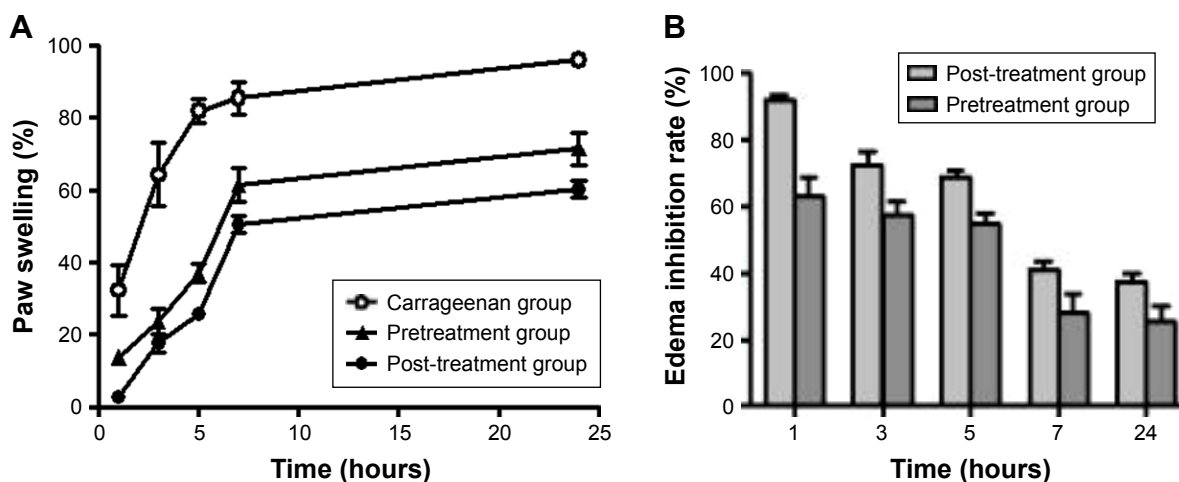


**Figure 8** Effect of once topical application of the medicated film.

**Notes:** (A) Paw swelling (%) and (B) edema inhibition rate (%) in carrageenan-induced rat paw edema model. Pretreatment group (treatment with the medicated film of area 1.77 cm<sup>2</sup> 5 hours prior to carrageenan injection). Post-treatment group (treatment with the medicated film of area 1.77 cm<sup>2</sup> after half an hour of carrageenan injection). Data are mean  $\pm$  SEM (n=6).

The paw swelling (%), edema inhibition rate (%), histologic examination, and IHC evaluation of COX-2 and NF- $\kappa$ B expression levels in rat paw edema tissues were recorded at three time intervals: 7, 14, and 24 hours.

#### Histologic evaluation of the anti-inflammatory effect of daily triple post-treatment regimen on rat paw edema tissue

Histologic examination displayed a marked reduction in paw tissue inflammation involving skin (Figure 9) and muscles (Figure 10) in post-treatment regimen at three time intervals; 7, 14, and 24 hours comparably with paw tissue exposed to carrageenan alone.

Statistical analysis of inflammatory scores at 7, 14, and 24 hours is presented in Figure 11. Post-treatment

significantly decreased ( $p < 0.05$ ) the inflammatory scores at 7, 14, and 24 hours in comparison with paw tissues exposed to carrageenan alone. The inflammation scores in paw tissue appeared to be decreased by time, following post-treatment regimen.

#### IHC evaluation of expression levels of COX-2 and NF- $\kappa$ B in rat paw edema tissues

In the present study, IHC technique was accomplished to elucidate the anti-inflammatory activity of APO film via determination of the protein expression levels of NF- $\kappa$ B and a pro-inflammatory mediator COX-2 in rat paw edema tissues.

COX-2 represents a vital key enzyme in inflammation and is considered as a rate-limiting enzyme, which catalyzes

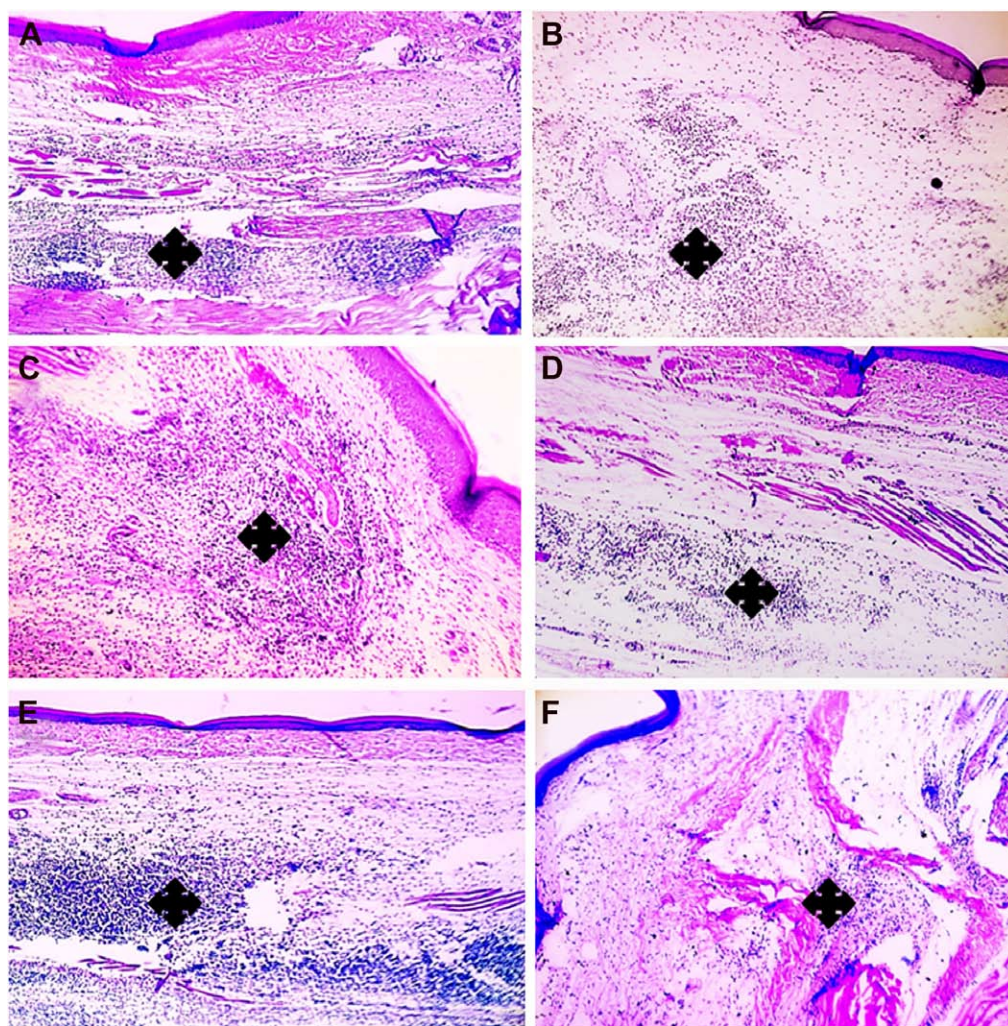


**Figure 9** Histologic evaluation of the anti-inflammatory effect of medicated film after triple application in carrageenan-induced rat paw edema model (dermis).

**Notes:** Left column (A, C, E) demonstrates paw tissue exposed to carrageenan alone, while right column (B, D, F) demonstrates post-treated paw tissues after triple application of the medicated film. (A, B) After 7 hours, (C, D) after 14 hours, and (E, F) after 24 hours. Marked reduction of inflammation in dermis (asterisks) is obvious in (B, D, F) when compared to (A, C, E). H&E, 100 $\times$ .

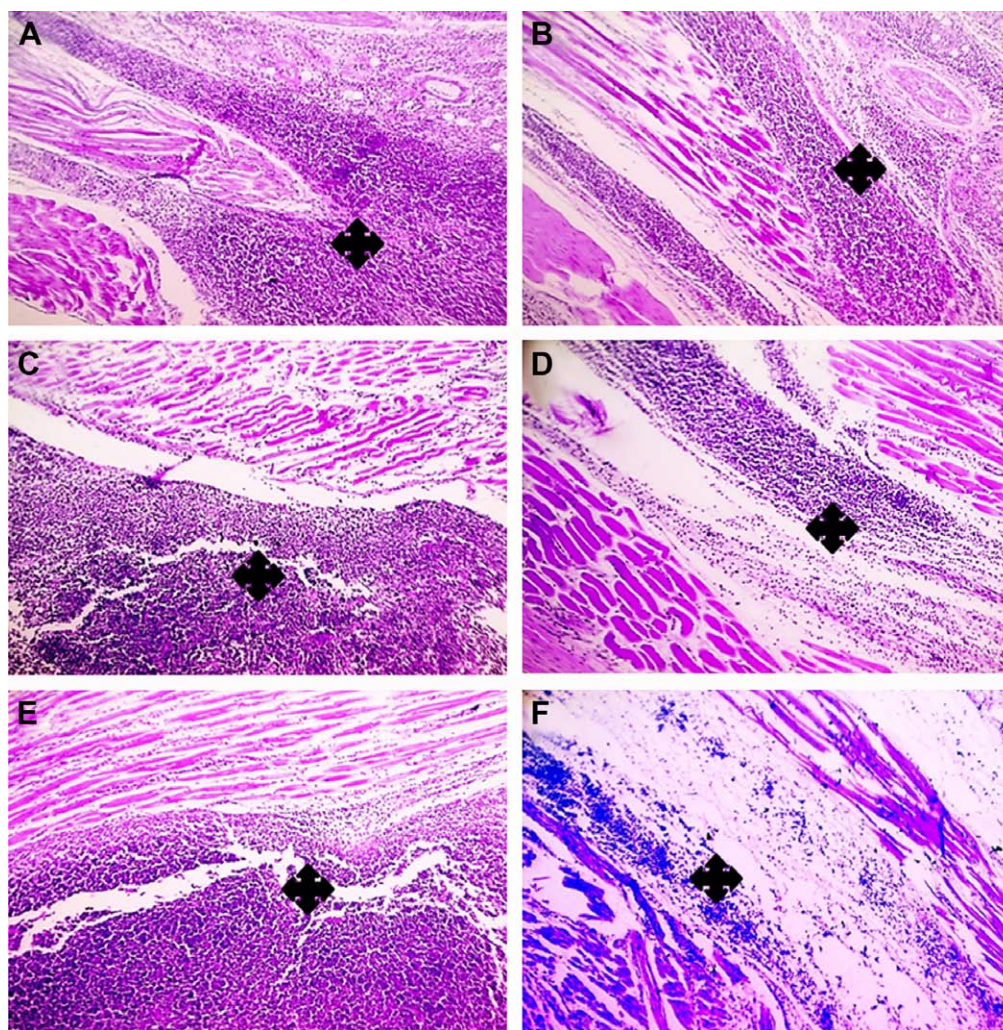


**Figure 10** Histologic evaluation of the anti-inflammatory effect of medicated film after triple application in carrageenan-induced rat paw edema model (muscle). **Notes:** Left column (A, C, E) demonstrates paw tissue exposed to carrageenan alone, while right column (B, D, F) demonstrates post-treated paw tissues after triple application of the medicated film. (A, B) After 7 hours, (C, D) after 14 hours, and (E, F) after 24 hours. Marked reduction of inflammation in muscle (asterisks) is obvious in (B, D, F) when compared to (A, C, E). H&E, 100 $\times$ .

prostaglandins production.<sup>44</sup> NF- $\kappa$ B is recognized to be the main transcription factor regulating the gene expression of numerous proinflammatory mediators like cytokines, growth factors, chemokines, and inducible enzymes. Hence, its inhibition leads to reduction of inflammatory genes.<sup>45</sup>

Compared with paw tissues exposed to carrageenan alone, a prominent reduction in the immunostaining of COX-2 was observed in paw tissues treated with APO film at three time intervals: 7, 14, and 24 hours, as shown in Figure 12 at 100 $\times$ . Similar findings were detected with NF- $\kappa$ B (Figure 13). Higher magnification (200 $\times$ ) for immunohistochemistry of both COX-2 and NF- $\kappa$ B is illustrated in Figures S5 and S6. Statistical analyses of positive signal expression of both COX-2 and NF- $\kappa$ B disclosed their significant decrease ( $p < 0.05$ ) after post-triple application of APO film when

compared to carrageenan alone (Figure 14). In addition, this effect seemed to be time dependent. These data could assume the involvement of COX-2 and NF- $\kappa$ B inhibition in the anti-inflammatory activity of APO film.

These promising data are greatly supported by the previously reported anti-inflammatory activity of APO in diverse cell lines and experimental animal models of inflammation. For instance, Hwang et al<sup>10</sup> elucidated the anti-inflammatory mechanism of APO against lipopolysaccharide-induced inflammation in RAW264.7 macrophage cells by prohibiting the nuclear translocation of NF- $\kappa$ B and suppressing the expression of COX-2, nitric oxide (NO), tumor necrosis factor- $\alpha$ , and prostaglandin E<sub>2</sub>, as well as proinflammatory cytokines. Also, APO abrogated COX-2 expression in human adherent monocytes subjected to serum-treated

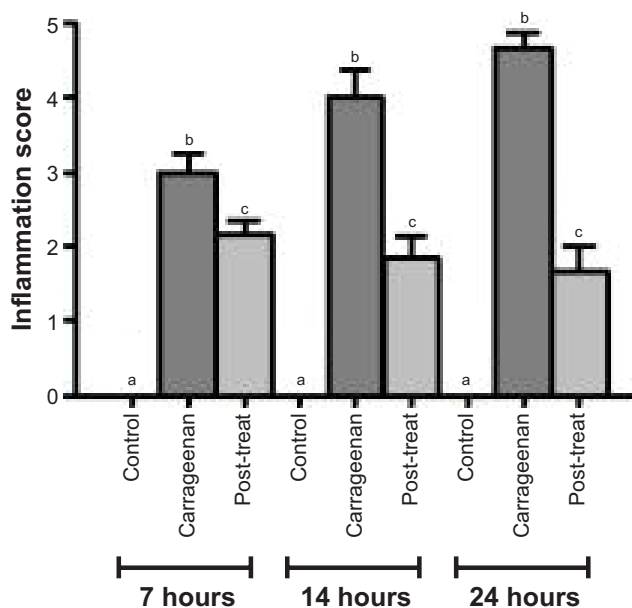


**Figure 11** Statistical analysis of inflammatory scores in H&E-stained paw tissues in control and carrageenan-alone groups as well as post-treated group following triple application of the medicated film.

**Notes:** Data are mean  $\pm$  SEM ( $n=6$ ). Different small letters (a–c) within each time interval indicate significance when  $P<0.05$ .

zymosan and phorbol myristate acetate via NADPH oxidase and glutathione redox-dependent mechanisms.<sup>46</sup> Thence, such influence might supply extra explication for the in vivo anti-inflammatory effect of the drug.

Other investigators demonstrated that oral administration of APO promoted a significant decrease in ear swelling and inhibition of COX in zymosan-induced inflammation of mice ears.<sup>7</sup> As well, they indicated the partial restoration of diminished synthesis of cartilage proteoglycan in arthritis mice model induced by zymosan following orally administered APO. Collectively, their data reflected the potential therapeutic effect of APO in chronic inflammatory joint disorders like rheumatoid arthritis and osteoarthritis. The capability of APO to diminish COX-2 expression in vivo might explain the anti-inflammatory effect of the drug in ameliorating joint swelling and ulcerative skin lesions in collagen-induced arthritis in mice and inflamed skin in rats, respectively.<sup>5</sup> Noteworthy, APO approval safety over long-term administration is encouraging enough to warrant further study on formulation of new dosage forms.<sup>47</sup>

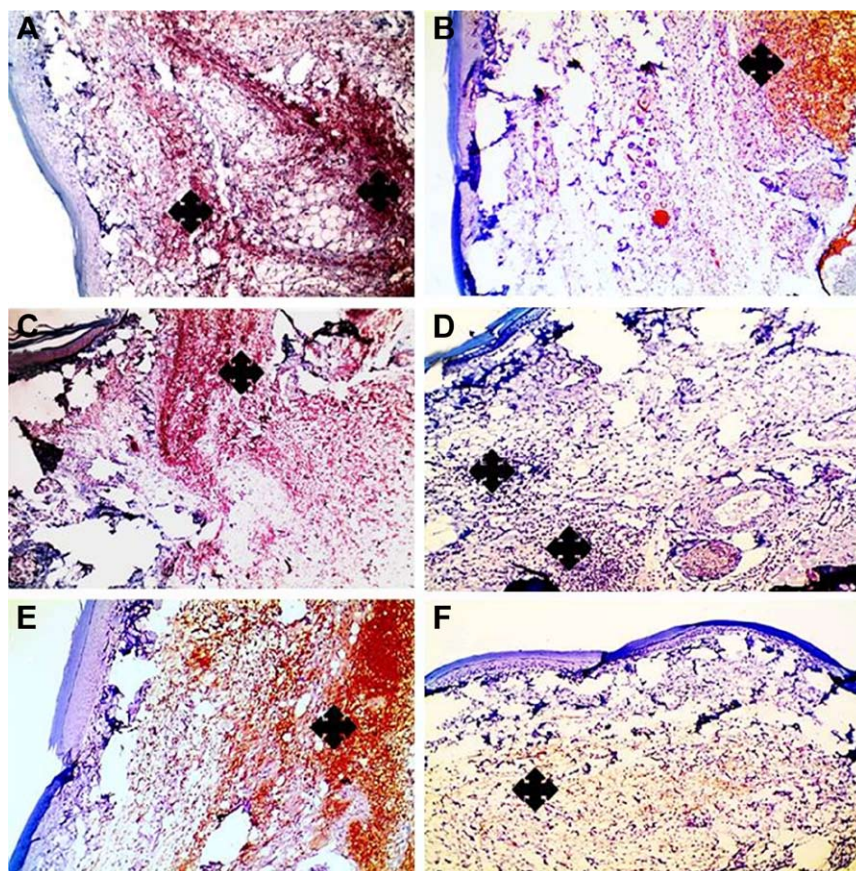


**Figure 12** Positive signal for IHC staining of COX-2 in rat paw tissue.

**Notes:** Left column (A, C, E) demonstrates paw tissue exposed to carrageenan alone, while right column (B, D, F) demonstrates post-treated paw tissues after triple application of the medicated film. (A, B) After 7 hours, (C, D) after 14 hours, and (E, F) after 24 hours. Marked reduction of positive signal in paw tissues (asterisks) is obvious in (B, D, F) when compared to (A, C, E). IHC counterstained with Mayer's hematoxylin, 100 $\times$ .

**Abbreviations:** COX-2, cyclooxygenase-2; IHC, immunohistochemical.

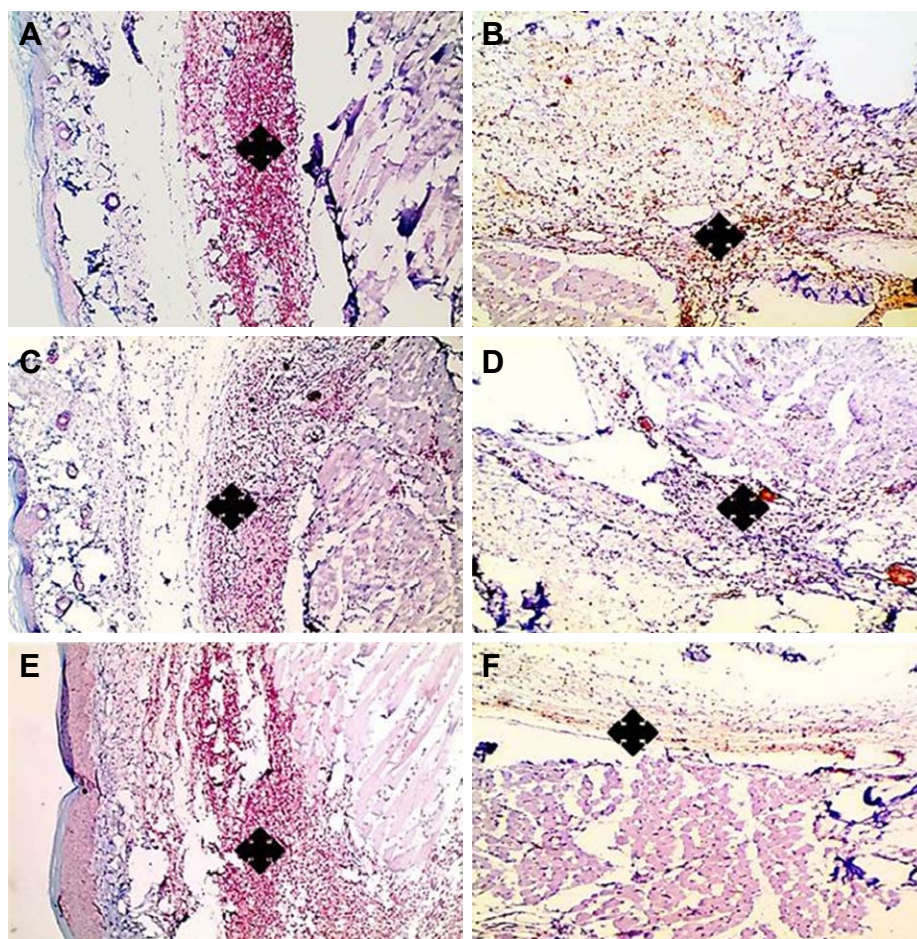


**Figure 13** Positive signal for IHC staining of NF- $\kappa$ B in rat paw tissue.

**Notes:** Left column (A, C, E) demonstrates paw tissue exposed to carrageenan alone, while right column (B, D, F) demonstrates post-treated paw tissues after triple application of the medicated film. (A, B) After 7 hours, (C, D) after 14 hours, and (E, F) after 24 hours. Marked reduction of positive signal in paw tissues (asterisks) is obvious in (B, D, F) when compared to (A, C, E). IHC counterstained with Mayer's hematoxylin, 100 $\times$ .

**Abbreviations:** IHC, immunohistochemical; NF- $\kappa$ B, nuclear factor kappa B.

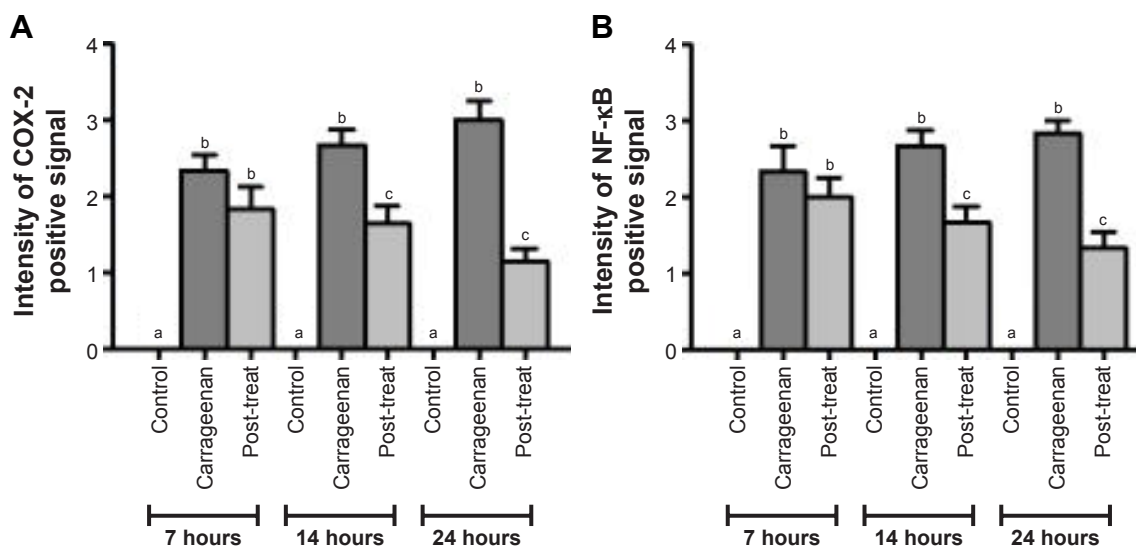


**Figure 14** Statistical analysis of intensity of positive signal.

**Notes:** (A) COX-2- and (B) NF- $\kappa$ B-stained paw tissues in control and carrageenan-alone groups as well as post-treated group following triple application of the medicated film. Data are mean  $\pm$  SEM (n=6). Different small letters (a-c) within each time interval indicate significance when  $P < 0.05$ .

**Abbreviations:** COX-2, cyclooxygenase-2; NF- $\kappa$ B, nuclear factor kappa B.

## Conclusion

In the current research, we focused on exploiting the tremendous benefits of APO, a specific NADPH-oxidase inhibitor, and CAS, a protein film former, as natural biocomponents to develop novel anti-inflammatory topical film. The medicated film exhibited satisfactory data regarding its physicochemical properties, ex vivo permeation profile, and stability. Post-treatment regimen with topical APO film provoked a prominent in vivo anti-inflammatory activity on carrageenan-induced rat paw edema model that was emphasized by histopathologic examination and IHC evaluation. The film can be applied in case of pressure ulcer, wounds, and burns. In summary, this study highlights the prospective topical application of CAS film loaded with APO for management of inflammatory disorders.

## Disclosure

The authors report no conflicts of interest in this work.

## References

- Lawrence T, Fong C. The resolution of inflammation: anti-inflammatory roles for NF-kappaB. *Int J Biochem Cell Biol.* 2010;42(4):519–523.
- Curtis JR, Westfall AO, Allison J, et al. Population-based assessment of adverse events associated with long-term glucocorticoid use. *Arthritis Rheum.* 2006;55(3):420–426.
- Sinha M, Gautam L, Shukla PK, Kaur P, Sharma S, Singh TP. Current perspectives in NSAID-induced gastropathy. *Mediators Inflamm.* 2013; 2013:1–11. ID 258209.
- Haroutiunian S, Drennan DA, Lipman AG. Topical NSAID therapy for musculoskeletal pain. *Pain Med.* 2010;11(4):535–549.
- Stefanska J, Pawliczak R. Apocynin: molecular aptitudes. *Mediators Inflamm.* 2008;2008:1–10; ID 106507.
- Kinoshita H, Matsumura T, Ishii N, et al. Apocynin suppresses the progression of atherosclerosis in apoE-deficient mice by inactivation of macrophages. *Biochem Biophys Res Commun.* 2013;431(2):124–130.
- Hougee S, Hartog A, Sanders A, et al. Oral administration of the NADPH-oxidase inhibitor apocynin partially restores diminished cartilage proteoglycan synthesis and reduces inflammation in mice. *Eur J Pharmacol.* 2006;531(1–3):264–269.
- Fan R, Shan X, Qian H, et al. Protective effect of apocynin in an established alcoholic steatohepatitis rat model. *Immunopharmacol Immunotoxicol.* 2012;34(4):633–638.
- Marin M, Giner RM, Ríos JL, Recio Mdel C. Protective effect of apocynin in a mouse model of chemically-induced colitis. *Planta Med.* 2013; 79(15):1392–1400.
- Hwang Y-J, Lee SJ, Park J-Y, et al. Apocynin suppresses lipopolysaccharide-induced inflammatory responses through the inhibition of MAP kinase signaling pathway in RAW264.7 cells. *Drug Dev Res.* 2016;77(6):271–277.
- Ximenes VF, Kanegae MP, Rissato SR, Galliane MS. The oxidation of apocynin catalyzed by myeloperoxidase: proposal for NADPH oxidase inhibition. *Arch Biochem Biophys.* 2007;457(2):134–141.
- Karki S, Kim H, Na S-J, Shin D, Jo K, Lee J. Thin films as an emerging platform for drug delivery. *AJPS.* 2016;11(5):559–574.
- Livney YD. Milk proteins as vehicles for bioactives. *Curr Opin Colloid Interface Sci.* 2010;15(1–2):73–83.
- Swaisgood HE. Chemistry of the caseins. In: Fox PF, McSweeney PLH, editors. *Advanced Dairy Chemistry. Vol. 1: Proteins Part A.* New York: Kluwer Academic/Plenum Publishers; 2003:139–202.
- Elzoghby AO, El-Fotoh WS, Elgindy NA. Casein-based formulations as promising controlled release drug delivery systems. *J Control Release.* 2011;153(3):206–216.
- Bajpai SK, Shah FF, Bajpai M. Dynamic release of gentamicin sulfate (GS) from alginate dialdehyde (AD)-crosslinked casein (CAS) films for antimicrobial applications. *Des Monomers Polym.* 2016;20(1): 18–32.
- Balaji A, Krishnaveni B, Goud V. Formulation and evaluation of mucoadhesive buccal films of atorvastatin using natural protein. *Int J Pharm Pharm Sci.* 2014;6(2):332–337.
- El-Setouhy DA, Abd El-Malak NS. Formulation of a novel tianeptine sodium orodispersible film. *AAPS Pharm Sci Tech.* 2010; 11(3):1018–1025.
- Allam A, Fetih G. Sublingual fast dissolving niosomal films for enhanced bioavailability and prolonged effect of metoprolol tartrate. *Drug Des Devel Ther.* 2016;10:2421–2433.
- Nafee NA, Boraie MA, Ismail FA, Mortada LM. Design and characterization of mucoadhesive buccal patches containing cetylpyridium chloride. *Acta Pharm.* 2003;53(3):199–212.
- Adhikari SNR, Nayak BS, Nayak AK, Mohanty B. Formulation and evaluation of buccal patches for delivery of atenolol. *AAPS Pharm Sci Tech.* 2010;11(3):1038–1044.
- Ubaidulla U, Reddy MVS, Ruckmani K, Ahmad FJ, Khar RK. Transdermal therapeutic system of carvedilol: effect of hydrophilic and hydrophobic matrix on in vitro and in vivo characteristics. *AAPS Pharm Sci Tech.* 2007;8(1):E13–E20.
- Bajpai SK, Bajpai M, Shah FF. Alginate dialdehyde (AD)-crosslinked casein films: synthesis, characterization and water absorption behavior. *Des Monomers Polym.* 2016;19(5):406–419.
- Abdellatif AA, Tawfeek HM. Transfersomal nanoparticles for enhanced transdermal delivery of clindamycin. *AAPS Pharm Sci Tech.* 2016;17(5):1067–1074.
- Higuchi T. Mechanism of sustained-action medication. Theoretical analysis of rate of release of solid drugs dispersed in solid matrices. *J Pharm Sci.* 1963;52(12):1145–1149.
- Korsmeyer RW, Gurny R, Doelker E, Buri P, Peppas NA. Mechanisms of solute release from porous hydrophilic polymers. *Int J Pharm.* 1983; 15(1):25–35.
- Namdeo A, Jain NK. Liquid crystalline pharmacogel based enhanced transdermal delivery of propranolol hydrochloride. *J Control Release.* 2002;82(2–3):223–236.
- Necas J, Bartosikova L. Carrageenan: a review. *Vet Med.* 2013;58(4): 187–205.
- Naito Y, Yasumuro M, Kondou K, Ohara N. Antiinflammatory effect of topically applied propolis extract in carrageenan-induced rat hind paw edema. *Phytother Res.* 2007;21(5):452–456.
- Bancroft JD, Gamble M. *Theory and Practice of Histological Techniques.* 5th ed. London, UK: Churchill Livingstone; 2007.
- Bang JS, Oh DH, Choi HM, et al. Anti-inflammatory and antiarthritic effects of piperine in human interleukin 1 $\beta$ -stimulated fibroblast-like synoviocytes and in rat arthritis models. *Arthritis Res Ther.* 2009; 11(2):R49.
- Hussein SZ, Mohd Yusoff K, Makpol S, Mohd Yusof YA. Gelam honey attenuates carrageenan-induced rat paw inflammation via NF- $\kappa$ B pathway. *PLoS One.* 2013;8(8):e72365.
- Fisher ER, Anderson S, Dean S, et al. Solving the dilemma of the immunohistochemical and other methods used for scoring estrogen receptor and progesterone receptor in patients with invasive breast carcinoma. *Cancer.* 2005;103(1):164–173.
- Charan J, Kantharia ND. How to calculate sample size in animal studies? *J Pharmacol Pharmacother.* 2013;4(4):303–306.
- Björklund S, Engblom J, Thuresson K, Sparr E. Glycerol and urea can be used to increase skin permeability in reduced hydration conditions. *Eur J Pharm Sci.* 2013;50(5):638–645.
- Ghosh A, Ali MA, Dias GJ. Effect of cross-linking on microstructure and physical performance of casein protein. *Biomacromolecules.* 2009; 10(7):1681–1688.

37. Schmid-Wendtner M-H, Korting HC. The pH of the skin surface and its impact on the barrier function. *Skin Pharmacol Physiol*. 2006;19(6): 296–302.
38. Bonnaillie LM, Zhang H, Akkurt S, Yam KL, Tomasula PM. Casein films: the effects of formulation, environmental conditions and the addition of citric pectin on the structure and mechanical properties. *Polymers*. 2014;6(7):2018–2036.
39. Rowe RC, Sheskey PJ, Weller PJ. *Handbook of Pharmaceutical Exipients*. 4th ed. London: The Pharmaceutical Press; Washington: American Pharmaceutical Association; 2003.
40. Dong Q, Hsieh Y-L. Acrylonitrile graft copolymerization of casein proteins for enhanced solubility and thermal properties. *J Appl Polym Sci*. 2000;77(11):2543–2551.
41. Elzoghby AO, Samy WM, Elgindy NA. Novel spray-dried genipin-crosslinked casein nanoparticles for prolonged release of alfuzosin hydrochloride. *Pharm Res*. 2013;30(2):512–522.
42. Tagwireyi D, Majinda RR. Isolation and identification of acetovanillone from an extract of *Boophone disticha* (L.f.) herb (Amaryllidaceae). *S Afr J Bot*. 2017;108:100–101.
43. Singh A, Bajpai J, Bajpai AK. Investigation of magnetically controlled water intake behavior of iron oxide impregnated superparamagnetic casein nanoparticles (IOICNPs). *J Nanobiotechnol*. 2014;12(1): 38–44.
44. Rouzer CA, Marnett LJ. Cyclooxygenases: structural and functional insights. *J Lipid Res*. 2009;50(Suppl):S29–S34.
45. Lawrence T. The nuclear factor NF- $\kappa$ B pathway in inflammation. *Cold Spring Harb Perspect Biol*. 2009;1(6):a001651.
46. Barbieri SS, Cavalca V, Eligini S, et al. Apocynin prevents cyclooxygenase 2 expression in human monocytes through NADPH oxidase and glutathione redox-dependent mechanisms. *Free Radic Biol Med*. 2004;37(2):156–165.
47. 't Hart BA, Copray S, Philippens I. Apocynin, a low molecular oral treatment for neurodegenerative disease. *Biomed Res Int*. 2014; 2014:1–6. ID 298020.

## Supplementary materials

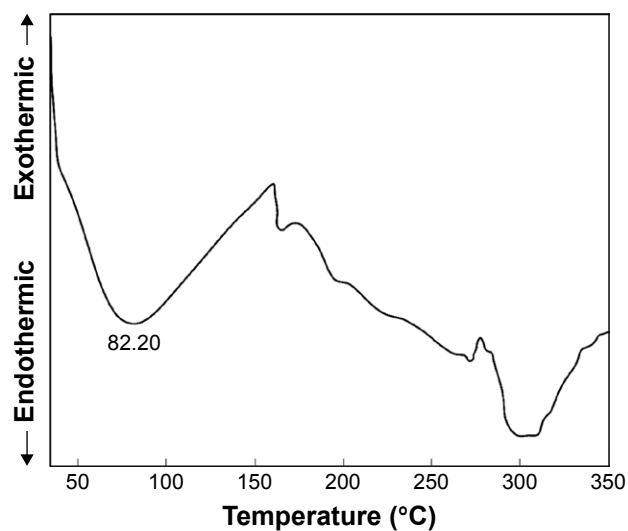


**Figure S1** Differential scanning calorimetry thermogram of plain film without glycerol.

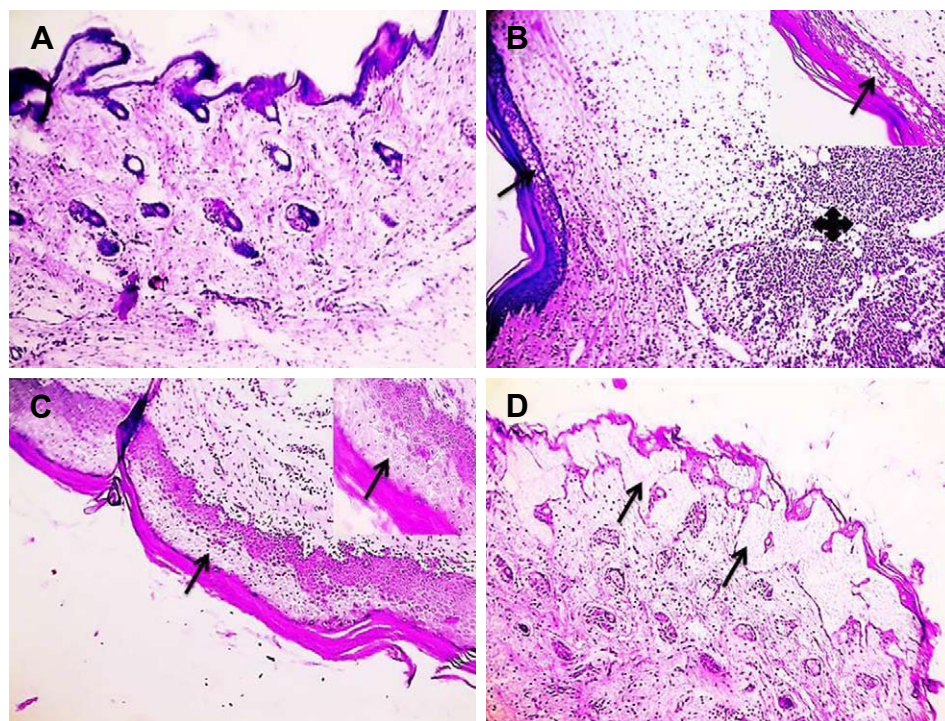


**Figure S2** Degenerative steps in paw tissue after carrageenan injection: (A) normal histology in control group, (B) vacuolar degeneration in epidermal cells (arrow) with severe inflammatory reaction in dermis (asterisk) after 7 h (insert is higher magnification, 200 $\times$ ), (C) hydropic degeneration in epidermal cells (arrow) after 7 h (insert is higher magnification, 200 $\times$ ), and (D) blisters formation (arrows) after 24 h. H&E, A–D 100 $\times$ .

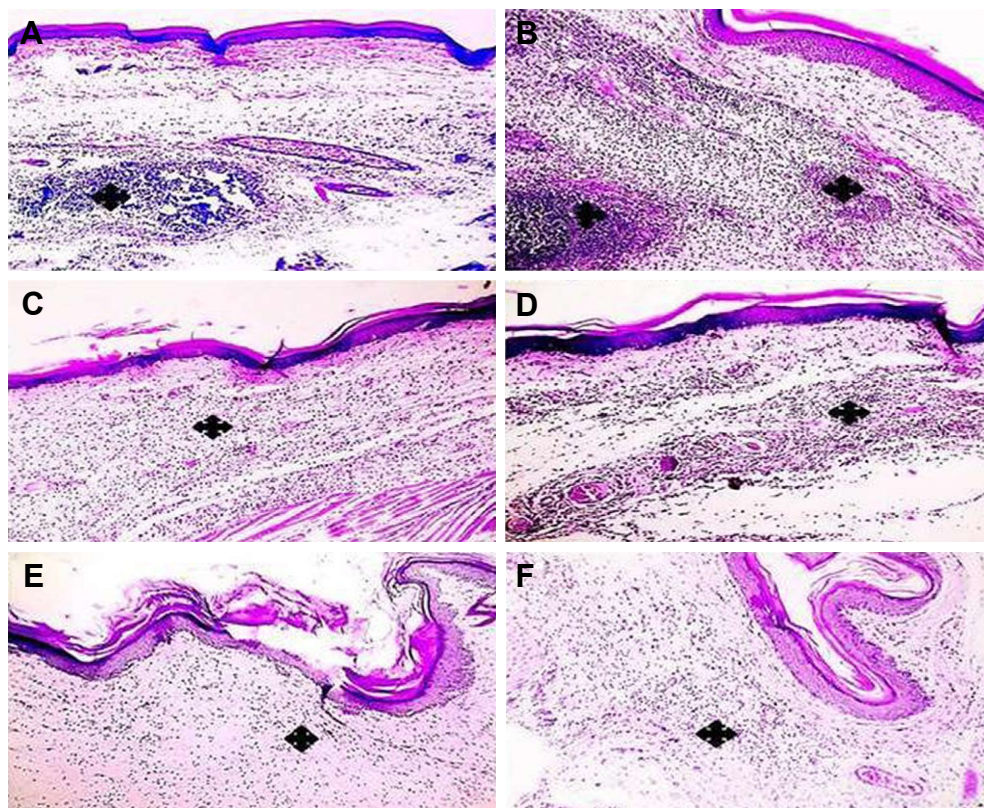


**Figure S3** Histologic evaluation of the anti-inflammatory effect of medicated film after once application in carrageenan-induced rat paw edema model.

**Notes:** Left column (A, C, E) demonstrates paw tissues of once application of the medicated film after 7 h carrageenan injection and right column (B, D, F) demonstrates paw tissues after 24 h carrageenan injection. (A, B) Paw tissues show massive accumulation of infiltrated neutrophils in paw tissue exposed to carrageenan alone (asterisks). (C–F) Paw tissue of treated groups shows milder inflammatory reactions. (C, D) Pretreated group (treatment with the medicated film of area 1.77 cm<sup>2</sup> 5 hours prior to carrageenan injection), (E, F) post-treated group (treatment with the medicated film of area 1.77 cm<sup>2</sup> after half an hour of carrageenan injection). H&E, 100 $\times$ .

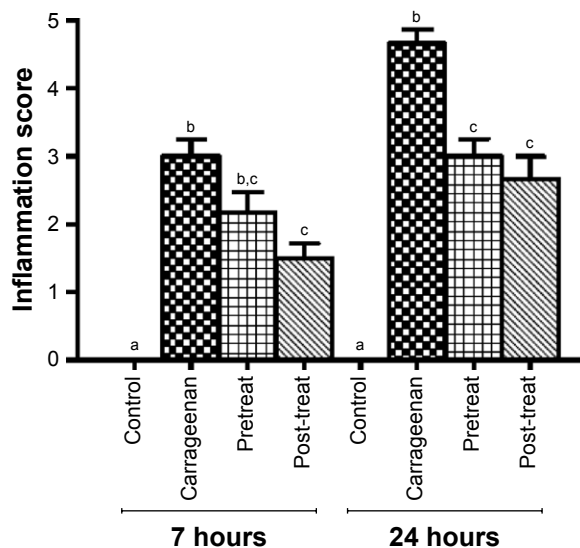


**Figure S4** Statistical analysis of inflammatory scores in H&E-stained paw tissues in control and carrageenan-alone groups (7 and 24 h) as well as pre- and post-treated groups following once application of the medicated film after 7 and 24 h carrageenan injection.

**Notes:** Pretreated group (treatment with the medicated film of area 1.77 cm<sup>2</sup> 5 hours prior to carrageenan injection) and post-treated group (treatment with the medicated film of area 1.77 cm<sup>2</sup> after half an hour of carrageenan injection). Data are mean  $\pm$  SEM (n=6). Different small letters (a–c) within each time interval indicate significance when  $P < 0.05$ .

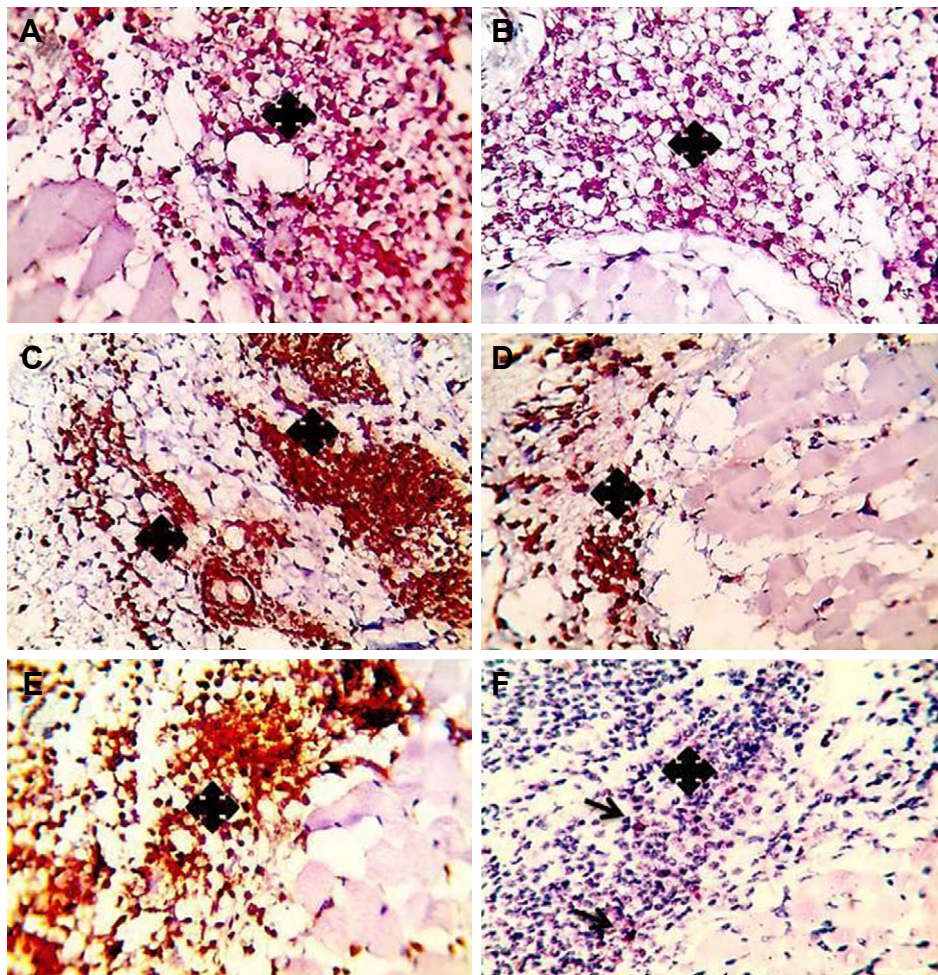


**Figure S5** Positive signal for IHC staining of cyclooxygenase-2 in paw tissue exposed to carrageenan alone as demonstrated in left column (**A, C, E**) and in post-treated paw tissues following triple application of the medicated film as demonstrated in right column (**B, D, F**). (**A, B**) After 7 h, (**C, D**) 14 h, and (**E, F**) 24 h. Marked reduction of positive signal in paw tissues (asterisks, arrows) is obvious in (**B, D, F**) when compared to (**A, C, E**). IHC counterstained with Mayer's hematoxylin, 200 $\times$ .

**Abbreviation:** IHC, immunohistochemical.

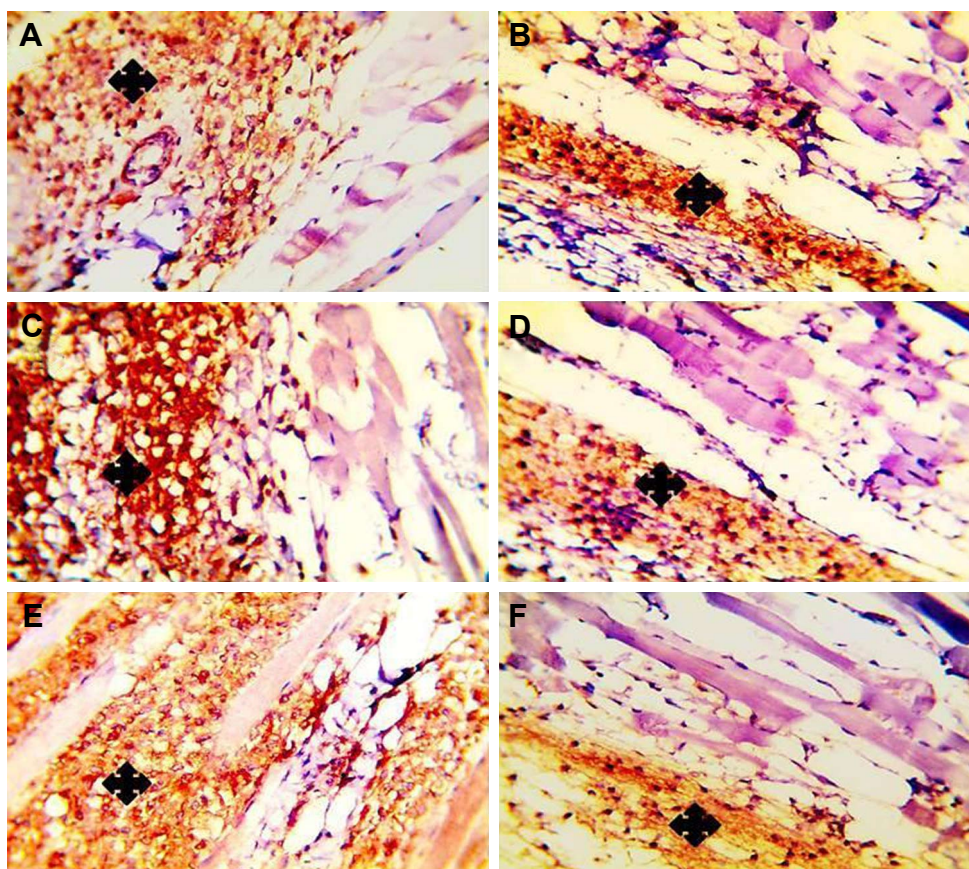


**Figure S6** Positive signal for IHC staining of nuclear factor kappa B in paw tissue exposed to carrageenan alone as demonstrated in left column (**A, C, E**) and in post-treated paw tissues following triple application of the medicated film as demonstrated in right column (**B, D, F**). (**A, B**) After 7 h, (**C, D**) 14 h, and (**E, F**) 24 h. Marked reduction of positive signal in paw tissues (asterisks) is obvious in (**B, D, F**) when compared to (**A, C, E**). IHC counterstained with Mayer's hematoxylin, 200 $\times$ .

**Abbreviation:** IHC, immunohistochemical.

### Drug Design, Development and Therapy

#### Publish your work in this journal

Drug Design, Development and Therapy is an international, peer-reviewed open-access journal that spans the spectrum of drug design and development through to clinical applications. Clinical outcomes, patient safety, and programs for the development and effective, safe, and sustained use of medicines are the features of the journal, which

Submit your manuscript here: <http://www.dovepress.com/drug-design-development-and-therapy-journal>

Dovepress

has also been accepted for indexing on PubMed Central. The manuscript management system is completely online and includes a very quick and fair peer-review system, which is all easy to use. Visit <http://www.dovepress.com/testimonials.php> to read real quotes from published authors.